Int. J. Multiphase Flow Vol. 17, No. 4, pp. 519–532, 1991
Printed in Great Britain.

0301-9322/91 $3.00 + 0.00

ON THE MEASUREMENT AND MECHANISM OF DRYOUT IN VOLUMETRICALLY HEATED COARSE PARTICLE BEDS

K. HU and T. G. THEOFANOUS†
School of Nuclear Engineering, Purdue University, West Lafayette, IN 47907, U.S.A.

(Received 1 March 1986; in revised form 1 March 1991)

Abstract—Experimental data, obtained at Purdue's Large Scale Corium Bed Simulation Facility, indicate that the dryout delay time (DDT) is simply related to the applied power. The relationship, called the constant energy line (CEL), is useful to uniquely define the critical heat flux, q_{cr}. It also provides a convenient and highly accurate means for the experimental measurement of q_{cr}. Based on these data the Theofanous–Saito correlation is recommended for the prediction of q_{cr} in deep beds of non-spherical coarsely-sized particulates. Finally, a plausible, mechanistic, model of the pre-dryout transient, considering coolant depletion phenomena and flooding limitations, was developed to analytically demonstrate the CEL behavior.

Key Words: dryout, flooding, porous media, two-phase flow, coolability, debris bed coolability

1. INTRODUCTION

The problem of coolability of top flooded volumetrically heated, coarse particle beds ($d > 1$ mm) has received considerable attention in connection with LWR accident assessements (Commonwealth Edison Company 1981; Theofanous & Saito 1981). Non-coolable beds on the containment floor basemat imply penetration and non-condensible (including combustible components) gas generation; while coolability implies quenching of the corium debris and continuing steaming into the containment atmosphere. Clearly, both the mode of containment failure, as well as its likelihood, and timing, will vary depending on these two different phenomenological behaviors. The practical problem in reactor safety assessments, is complicated by the possibility of large bed non-uniformities and associated multidimensional effects. Still, useful perspectives may be gained by considering beds of uniform packing.

The coolability limit refers to a condition of maximum energy deposition, and removal by steaming, while all portions of the bed remain wetted. It is expressed as a critical heat flux (CHF), q_{cr}, based on the bed cross-sectional area, and it is understood that exceeding it will lead to the development of dryout areas within the bed. Theoretical work has reached the consensus that the CHF is governed by the liquid–vapor, counter-current flow limiting, process at the top layers of the bed. This limitation has been expressed either directly as a flooding limit [Theofanous & Saito (1981), Ostenson & Lipinski (1981) and Schrock *et al.* (1984), among others] or as a frictional coupling between the phases [Lipinski (1982), Marshall & Dhir (1983) and Dhir & Barleon (1981), among others]. The results are similar (Theofanous *et al.*, 1983) varying only in quantitative details, such as the form of relative permeabilities, the use of shape factors, numerical coefficients and exponents in the flooding correlation etc. Schrock *et al.* (1984) have recently shown that the two approaches are indeed related. By one count (Lipinski 1983), no less than 20 predictive methods are available.

By contrast the experimental determination of q_{cr} has not been fully established yet. Limitations include:

(a) *Scarcity and scatter of available data.* As shown in figure 1, even for the relatively "clean" case of spherical particulates, reproducibility is poor both within, as well as among the various data sets. A highly erratic or poorly controllable physical process is suggested by these data. Moreover, these data indicate a rapidly increasing behavior above the flat plate CHF with increasing particle sizes beyond 5 mm.

†Current address: Department of Chemical and Nuclear Engineering, University of California, Santa Barbara, CA 93106, U.S.A.

(b) *Particle shape and bed dimensions.* Debris of any but spherical shape, and bed depths well over 40 cm are of interest for addressing the coolability of corium debris beds. Furthermore, depending on the particle size, an adequately large bed cross-sectional area must be chosen if wall effects (locally increased porosity and associated multidimensional effects) are to be minimized. Hu *et al.* (1984) and Hu & Theofanous (1986) have recently presented data from a facility designed to address these concerns. These data indicate a q_{cr} significantly below the data ranges shown in figure 1, but in agreement with the Theofanous–Saito correlation (see also section 3.3). However, additional clarifications of shape factors, and permeability corrections are necessary before all data and various predictive schemes can be compared on a consistent basis.

(c) *Measurements and mechanisms.* The experimental measurement of q_{cr} has been based on the understanding that a condition of $q > q_{cr}$ would lead to rapid dryout. Thus, in a typical experimental run the power was increased in small steps at short time intervals (1–2 min) until a temperature excursion was observed. Instead of local temperature excursions, Somerton *et al.* (1981) and Catton *et al.* (1983) have employed an integral measure: the time required to completely fill the bed with water after power is turned off. On the basis that this measure is related to the size of the dryout zone the limit of dryout inception (dryout zone approaching zero dimensions) was defined by the first departure of the refill time from that obtained at low power levels. Again, for $q > q_{cr}$, rapid dryout was assumed to occur, thus a power-on condition for 1–2 min was typically employed. A whole different perspective is suggested by Hofmann's work (Hofmann 1982; Hofmann & Schulenberg 1983). He reported dryout inception delays (after power application) as long as 1 h, and related analytically predicted saturation transients to visually observed flow patterns and the dryout inception event.

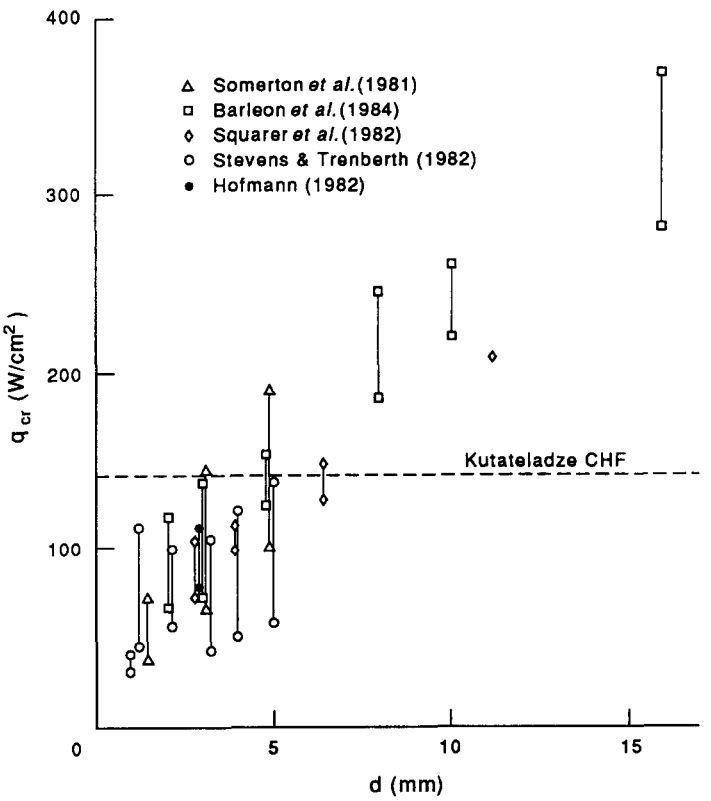

Figure 1. Available experimental data on debris bed coolability in the large particle regime. Water, 1 bar, $\epsilon \sim 0.4$.

The existence of long dryout delays was confirmed by Hu & Theofanous (1986) who discovered that for a given bed, fluid and operating pressure, the dryout delay time (DDT) is related to the applied power, q, by

$$(q - q_{cr}) \times \text{DDT} = E, \qquad [1]$$

where the energy change per unit area, E, is a constant. They proposed that on this basis q_{cr} can be *uniquely defined* as an asymptotic limit (i.e. yielding dryout after an infinitely long delay), and that this limit can be conveniently, and accurately, inferred from a few experimental runs, and resulting q-DDT pairs. For any other power level above this limit, dryout will occur with a time delay given by the above equation. The purpose of this paper is to provide thorough experimental support for this proposal. Referring to the areas of concern (a) and (b) above, the data are highly accurate and reproducible, and these are the first (only) data with a bed of irregular particle shapes and negligible wall effects. Referring to concern (c) above, a quantitative interpretation of the above-mentioned hyperbolic trend is developed and utilized to gain further insight into the definition of q_{cr} and its relationship to the dryout phenomena.

2. EXPERIMENTAL FACILITY

Experiments were carried out with Purdue's Large Scale Corium Bed Simulation Facility (Hu 1985). This facility employs a novel experimental technique for creating a volumetrically (or quasi-volumetrically) heated bed of arbitrary composition and dimensions. These dimensions are only limited by the available d.c. or a.c. power. In the present setup a variable 100 kW d.c. power generator is employed for a cylindrical bed 101.6 cm high and 21.6 cm dia. Thus, a peak power density of 2.7 W/cm^3 and a peak equivalent, bed surface, (top bed layer) flux of 273 W/cm^2 may be obtained.

The basic concept is to utilize electrical (resistance) heaters, threaded with aluminum spheres, and coiled in the manner shown in figure 2. These coils (heating elements) may be packed up to create a volumetrically heated bed of aluminum spheres. Alternatively, interdispersed layers of a particulate may be employed, as shown in figure 3, to create a quasi-uniformly heated bed of any desired particle and porosity characteristics. The data reported in this paper were obtained with

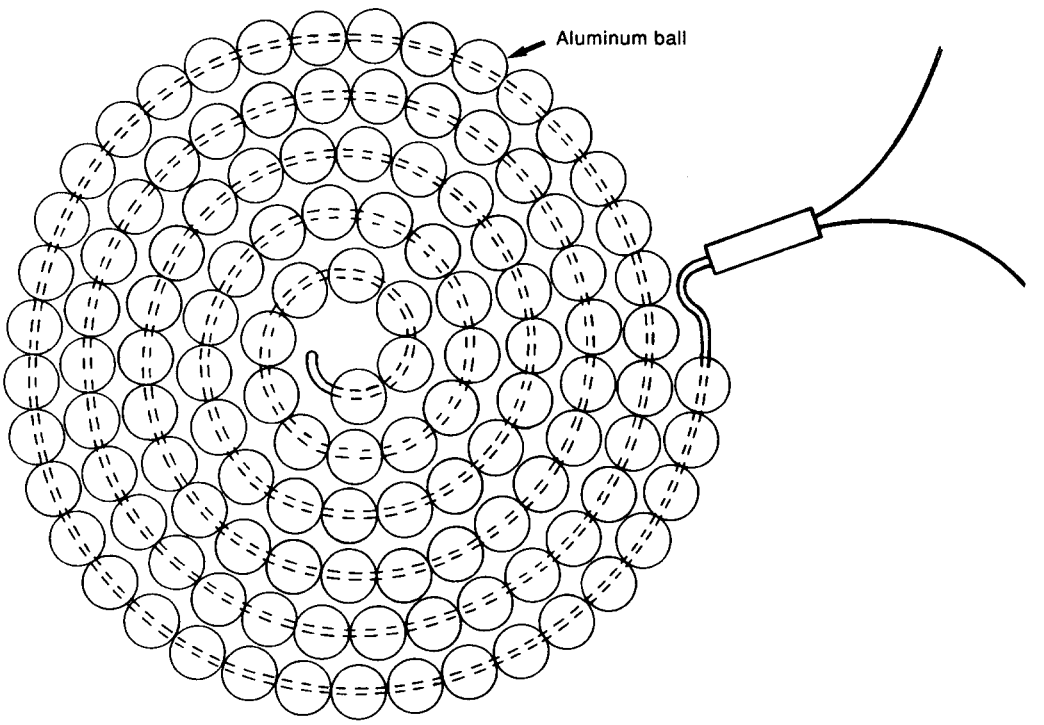

Figure 2. Schematic of a heating element.

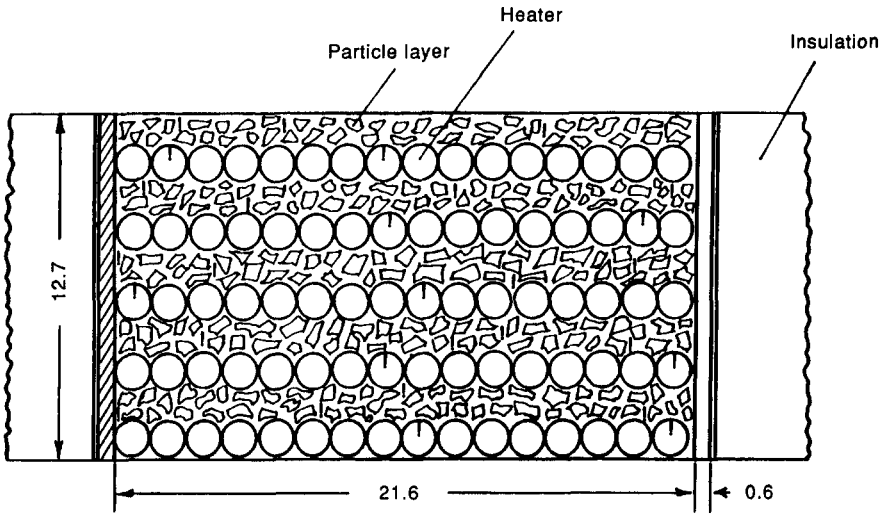

Figure 3. Debris bed module showing the internal structure. All dimensions in centimeters. Vertical dashes indicate thermocouple positions (30).

a bed made up with 1.25 cm aluminum spheres and stone gravel, with a characteristic dimension of ~8 mm (7–9 mm sieve pass). The aluminum/stone layers were in roughly equal proportions and a total of 40 such layers were employed. The container vessel was sectioned such that the bed could be assembled by attaching and packing one section (i.e. the module of figure 3) at a time. The whole assembly is shown in figure 4. Individual on–off power control is provided for each heater. For

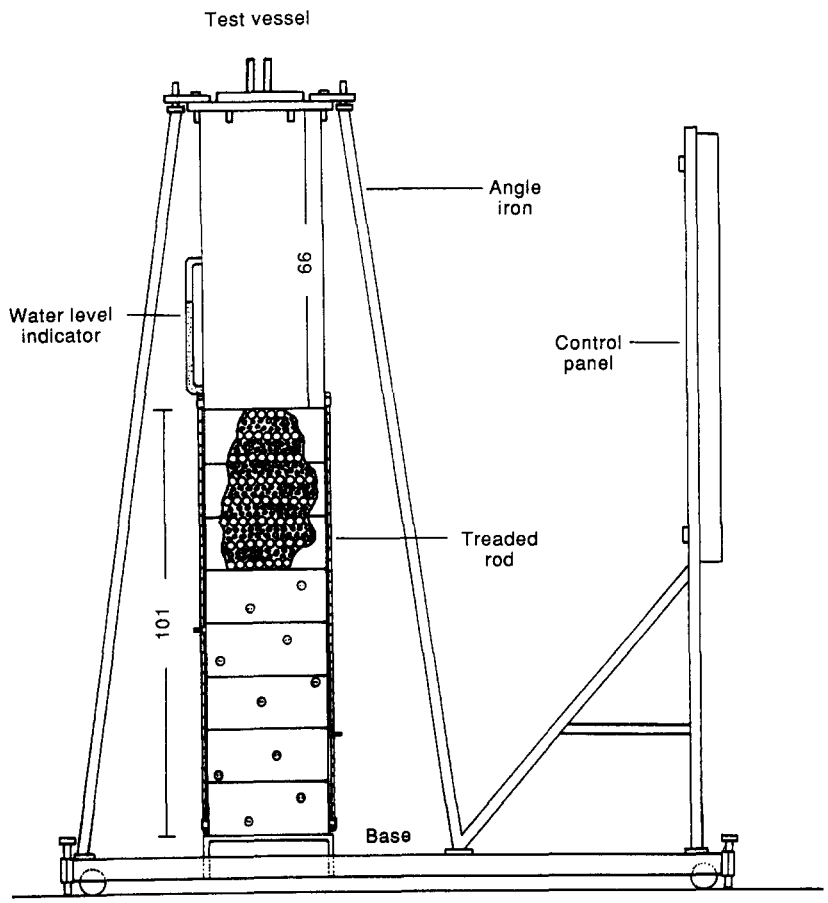

Figure 4. Schematic of the experimental facility. All dimensions in centimeters.

the peak condition mentioned in the previous paragraph, this bed would be subject to a local heat flux, on the surface of the aluminum spheres, of only 0.6 W/cm^2, thus no local overheating is possible in the presence of even very small quantities of water. The absence of such undesirable local effects was also confirmed by excellent reproducibility of the measured CHF in experiments employing only 20 heaters (every other heater was activated)—i.e. the same bed CHF for a locally (based on sphere surface area) double heat flux.

The liquid flooding level (submergence) is set within the 66-cm-long free-board volume formed by the last vessel section in the assembly. This section contains a copper condenser coil for coolant refluxing and it is equipped with an external sight glass for direct visual determination of the liquid level. The system has been designed for 0.69 MPa. With proper operation of the condenser, stable operation down to 48 kPa has been achieved. The vessel was well-insulated, as confirmed by the power input being within 0.5% of that removed by the condenser. However, the error in power input, as measured by the voltage and current applied to the heaters, was only $\pm 0.26\%$.

Two-hundred and forty Chromel–Alumel Teflon-sheathed ($d \sim 0.25$ mm) thermocouples were provided to measure temperatures throughout the bed. A PDP-11 process computer was employed to monitor the thermocouple outputs continuously (~ 4 s of scan time). All post-dryout temperature transients were recorded. In addition, an oscilloscope graphic display of the temperature scans was utilized as a convenient means of bed monitoring by the operator.

Special care was exercised for bed characterization. Its porosity was measured by the flooding method. Flooding under vacuum was followed by boiling (closed system in the reflux mode) to ensure the absence of an entrapped void space. The porosity values obtained, upon assembly, were 0.38 and 0.39, for the vacuum and boiling methods, respectively. Following a period of about 10 months of operation, a value of 0.387 was obtained by the vacuum method. The permeability was deduced from the volume throughput of water under ~ 60 cm of submergence. To ensure no exit losses the bottom plate of the test section was replaced with a heavy wire mesh. A value of 2.41×10^{-4} m was thus determined for permeability at turbulent flow. This compares well with the value of 1.5×10^{-4} m determined for another, small, bed formed only with the stone gravel from the same batch used in packing the large bed. It may, therefore, be concluded that, as intended, the permeability was controlled by the stone gravel, and the effect of the layering of the heater elements in between was to increase the permeability somewhat. The shape factor, expressing the actual surface area of a typical particle divided by the surface area of an equal-volume sphere, is expected to be ~ 1.24 (Gorham-Bergeron 1983).

3. EXPERIMENTAL RESULTS

3.1. The role of submergence

It has been suggested (Catton *et al.* 1983) that the excessive scatter in experimental values of q_{cr} (i.e. figure 1) is due to neglecting the role of bed submergence. Indeed, this potential parameter has rarely even been reported. Furthermore, Catton *et al.* (1983) have claimed that a submergence of >2.5 times the bed depth would be required for this parameter to cease being important.

In the first round of experimental data (Hu *et al.* 1984) from the present facility a bed submergence of ~ 25 cm (during boiling) was utilized. Tests of the effect of this parameter were subsequently conducted with a specially constructed top section of the experimental vessel allowing for ~ 91 cm (during boiling) of submergence. Reproducibility with the previous data was within 2%. We can conclude, therefore, that, at least for deep beds, the absolute magnitude of the submergence, rather than its value scaled by the bed depth is relevant, and that even a modest submergence of ~ 25 cm is quite adequate to prevent any extraneous effects. In all subsequent tests a submergence of ~ 25 cm was, therefore, employed.

3.2. The constant energy line (CEL)

Experimental runs for the determination of the dryout time were carried out as follows. Starting the bed at a fully saturated low-power-boiling condition the power was stepped (within a few seconds) to a level corresponding to a desired value of q, expected to exceed q_{cr}. The run continued

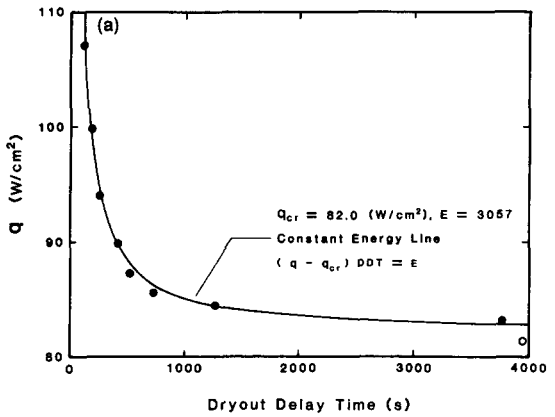

Figure 5a. Definition of q_{cr} in terms of the constant energy line. Each point represents a dryout inception run. The symbol ○ represents a power-time pair for which no dryout was observed. Water, 1 bar.

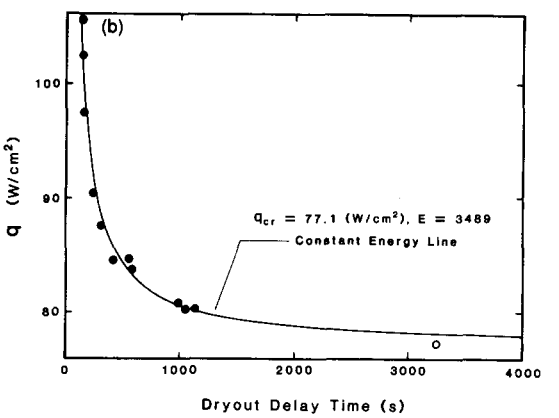

Figure 5b. Reproducibility of constant energy line about 5 months later. Water, 1 bar.

until the first temperature excursion† was detected, somewhere in the bed, by the monitoring systems. The time elapsed between the onset of q and the temperature excursion is called DDT. After the completion of one such run the power was reduced to very low levels ($\sim q_{cr}/2$). After a few minutes, to ensure complete return to fully wetted, saturated, low boiling conditions, the system was ready for another DDT measurement.

Results from two such sets of runs are shown in figures 5a and 5b. The data in both cases are well-fitted by a function in the form of [1]. This function we call the CEL. It is apparent that on this basis the determination of q_{cr} is unambiguous and highly accurate. It is important to note that these two data sets were obtained 5 months apart. The small difference in q_{cr} probably reflects the inherent experimental error in the present method. However, it could also be due, in part, to a slight change in the bed characteristics because of an intervening measurement of the permeability. This involved transportation of the whole bed to the outside, replacement of its base plate by a wire mesh, as already mentioned, and reassembly after the permeability measurement. The overall bed porosity, after this whole procedure, was found unchanged, nevertheless.

Additional data were obtained by enhancing the degree of power non-uniformity (due to the discrete layers of heaters) and with shorter heated bed depths. For the power non-uniformity tests power was supplied only to every other heating element. The results are shown in figure 6. The bed depth variation tests were carried out by supplying power only to the upper portions of the bed. To minimize downward heat losses the lower, unheated, portion of the bed was maintained to within 5°C below saturation. The results are shown in figure 7. A single CEL seems to describe, with excellent precision, all three of these data sets. Furthermore, the q_{cr} thus defined is in excellent agreement with that obtained from fully heated beds. These data clearly indicate that the quasi-uniform heating is not a factor, and within the range of bed depths investigated, the effect is not significant in causing local, dryout, effects.

3.3. Effects of ambient pressure

The effect of ambient pressure on q_{cr} has been quantified by Hu *et al.* (1984). The present facility was employed but at the time the CEL concept was unknown. The stepwise power increase procedure was therefore employed in those studies. The value of q_{cr} was assumed to be bracketed in the fashion shown in figure 8. The lower edge of each bracket indicates the power level for which no dryout was detected over the time period in minutes, shown at the side. The upper edge of each bracket indicates the power level to which the no-dryout, lower, condition was switched to, in order to achieve dryout. The time, in minutes, spent in this condition prior to dryout is also shown at the side. A rough re-evaluation of these original data may be offered in terms of the CEL concept.

†Continued operation yields successive excursions in nearby thermocouples, i.e. spreading of the dryout zone and escalation of the particle temperatures within it. The transient behavior observed may be found in Hu (1985).

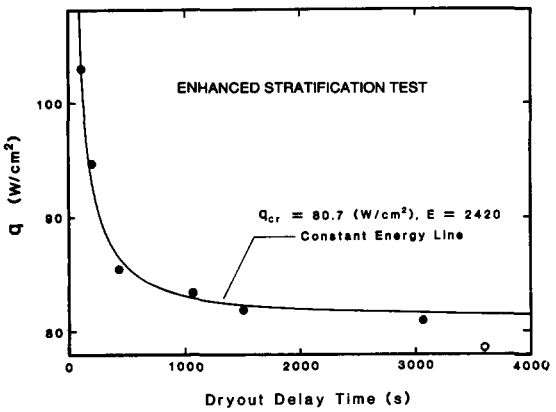

Figure 6. The measurement of q_{cr}, and demonstration of CEL behavior for an enhanced non-uniform pattern of heating: ● dryout; ○ no dryout. Water 1 bar.

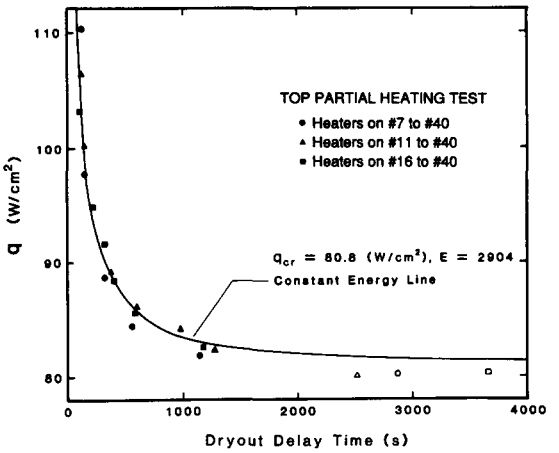

Figure 7. Insensitivity of q_{cr}, and CEL to various heated bed depths. Heater #40 is at the top. Open symbols represent the absence of dryout.

The approach is based on assuming that the CELs determined above are roughly applicable over the pressure range of these data (i.e. the E in [1] remains applicable). Now, if the power at the low end of each bracket was below q_{cr}, the q-DDT pairs at the upper ends could be used directly to determine q_{cr}. This is definitely true for the data at 1.00 and 2.35 bar; the resulting best estimate q values are shown in figure 8. Applications of this procedure to all other data results in q_{cr} values that are well below the q values of the lower ends, thus negating the starting hypothesis. Evidently, for these data the original data *did not* bracket q_{cr}. The best estimate for these cases may be obtained by assuming that the q at both ends of each bracket exceeded q_{cr}, while the point of operation (not shown) prior to these two successive power increases was below q_{cr}. The sum of the two times, may then roughly be considered the DDT corresponding to the average of the two power levels in order to calculate q_{cr} from [1]. The resulting values of q_{cr} are reported as best estimate values in figure 8.

Also, comparisons with two of the available prediction methods are shown in figure 8. Correction for the measured permeability is seen to significantly improve the prediction of Lipsinski's (1982) model. The Theofanous–Saito correlation, on the other hand, is based on a geometric shape factor

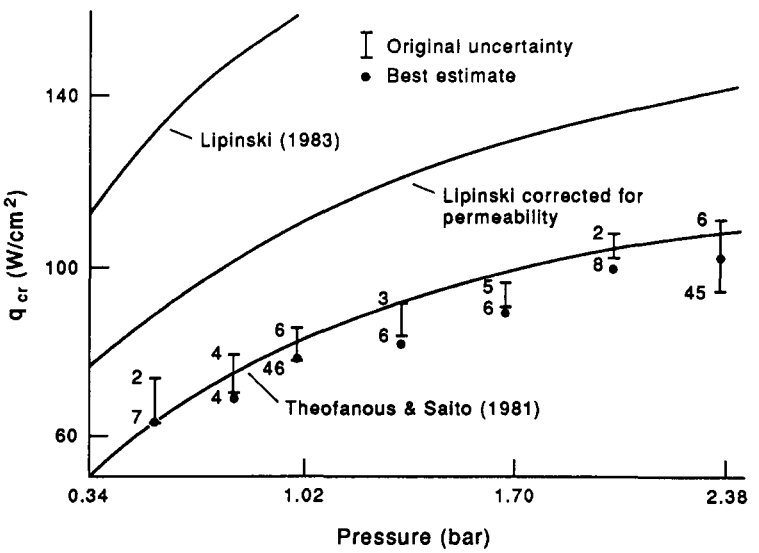

Figure 8. Variation of CHFs with pressure. The original uncertainty represents an attempt to bracket q_{cr} between a low value for which no dryout was observed over the time (in minutes) shown at the side, and an upper value for which dryout was observed, with a time delay shown (in minutes) at the side, after the change in power (Hu *et al.* 1984). The best estimate is derived from these times according to the CEL concept as described in the text. Water, 1 bar.

and the quoted value of 1.24 (Gorham-Bergeron 1983) seems to be adequate. Given the stone shapes such a value seems reasonable.

The comparison with previous data is shown in figure 9. In this plot the position of the present data can be referred to a spherical particle size of equal volume to the gravel (d_s), or (in a bed of many such particles) of equal permeability (d_p). In both interpretations the present data are well below the previous data base [with the possible exception of the data of Stevens & Trenberth (1982) depending on the interpretation of the ranges given], and well below the flat plate CHF. For spherical particle sizes of 4.7 mm, Catton *et al.* (1983) have measured values that exceeded the flat plate CHF by as much as a factor of 1.7! However, these data were obtained with a bed height of only 10 cm and a diameter of only 4.5 cm, using the reflooding technique mentioned in section 1. Thus, it is not clear whether the much higher (compared with prototypic values) power density, or the wall effects (large particles in a small diameter bed), or the experimental technique or some combination of them are responsible for this largely different behavior. In a slightly larger bed (6.1 cm dia) but with basically the same apparatus and technique, Jakobsson *et al.* (1983) have investigated the effect of pressure. They concluded that the flat plate CHF and Lipinski's model best predict the effect of pressure, and that Lipinski's model "generally" predicted the value of the dryout flux. Besides Zuber's CHF and Lipinski's model, these comparisons included the models/correlation of Sowa *et al.* (1971), Dhir & Catton (1977) and Dhir & Barleon (1981).

4. ANALYTICAL INTERPRETATION OF THE CEL

The form of [1] quite clearly implies a water depletion phenomenon. As a matter of fact we originally referred to it as a constant depletion line. The present analysis indicates that its relationship to depletion is rather complicated, thus the name CEL was deemed more appropriate. Our task is to analytically quantify DDT as a function of q and thus arrive at the CEL.

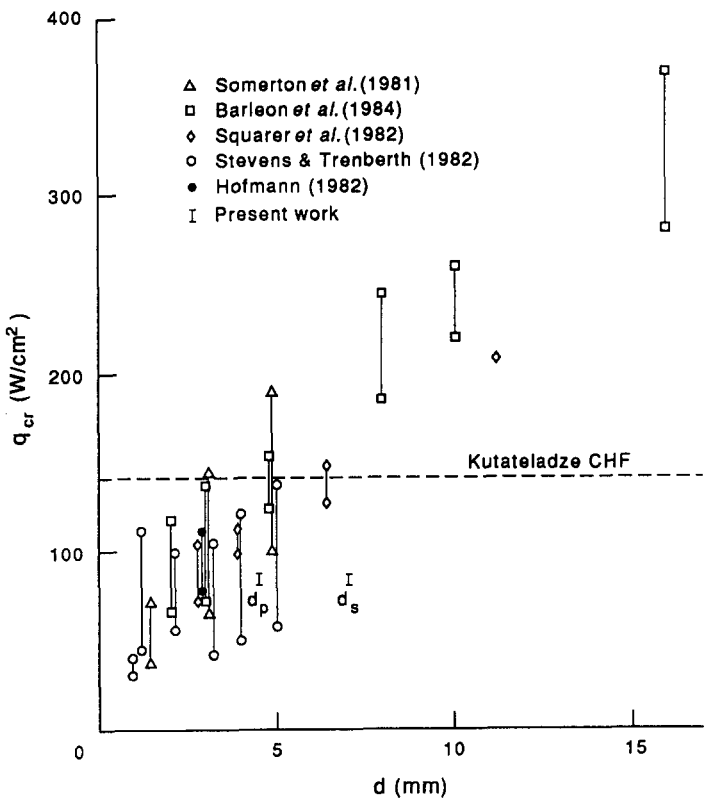

Figure 9. Comparison of the present data with the previous data base. d_s is the equivalent particle diameter based on an equal-volume sphere, and d_p is based on an equal permeability bed (of spheres).

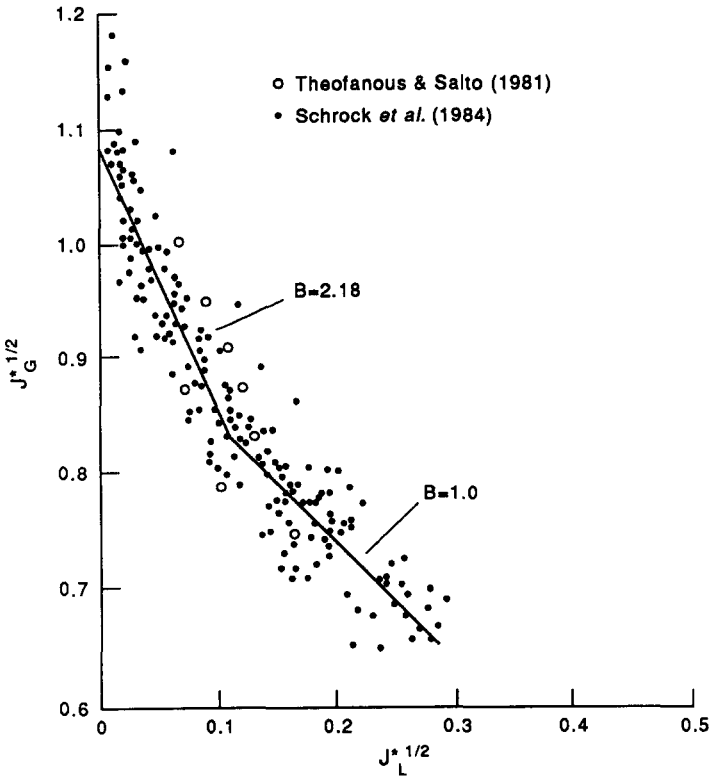

Figure 10. The flooding behavior at the low values of J_L^* pertinent to debris bed coolability; B is the absolute value of the slope of each line as indicated.

The calculation of DDT is based on estimating water depletion volumes, V_{Ld}, and associated water depletion rates, $\Delta m'$. These quantities are obtained along the general lines proposed by Hofmann (1982). That is, the water depletion volume is deduced from the change in the saturation profiles just after application of q and just before dryout, and the depletion rate is deduced from the imbalance between incoming liquid and outgoing vapor, caused by flooding, of the bed exit, for $q > q_{cr}$. However, quantitatively, several new elements seem to be necessary for arriving at a CEL.

4.1. The depletion rate

The water depletion rate, $\Delta m'$, within the bed may be obtained as the difference between the outgoing vapor mass flux and the incoming liquid mass flux:

$$\Delta m' = \rho_G J_G - \rho_L J_L. \quad [2]$$

The gas velocity, J_G, may be related to the heat flux input† by

$$q = \rho_G J_G h_{LG} \quad [3]$$

and the liquid velocity, J_L, may be related to J_G by the use of a flooding correlation. The relevant range for the present purposes is $0 < J_L^{*1/2} < 0.106$. The lower limit corresponds to zero liquid penetration and the upper limit to the condition of CHF. The gas/liquid flooding data of Theofanous & Saito (1981) and the steam/water data of Schrock *et al.* (1984) are summarized, for this range, in figure 10. The agreement between these two data sets appears reasonable and the slope, B, of the correlating line‡ in the low J_L^* range

$$J_G^{*1/2} + 2.18\, J_L^{*1.2} = C \quad [4]$$

†Prior to dryout all heat input goes to vapor production and the whole bed remains at saturation temperature.
‡This important, as it turns out, detail was not considered by Schrock *et al.* (1984).

is significantly higher than the value of ~ 1 generally accepted, as Wallis's correlation, over the broader J_L^* range. With the help of [3] and [4] and the definition of J_L^* and J_G^* [2] yields

$$\Delta m' = \begin{cases} \dfrac{q_{cr}}{h_{LG}}\left[1 - \dfrac{q_{cr}}{q}\left\{\dfrac{1}{2.18}\left(\dfrac{\rho_L}{\rho_G}\right)^{1/4}\left[1 - \left(\dfrac{q}{q_{cr}}\right)^{1/2}\right] + 1\right\}^2\right] & q > q_{cr} \\ 0 & q \leqslant q_{cr}. \end{cases} \quad [5]$$

The q_{cr} in the above equation is given by the Theofanous–Saito correlation

$$q_{cr} = 0.0707\,\rho_L h_{LG}\left[\frac{gd^3}{F(1-\epsilon)}\right]^{1/2}\left(\frac{\rho_G}{\rho_L}\right)^{5/8}\left(\frac{\mu_w}{\mu_L}\right)^{0.1}, \quad [6]$$

where ρ is density, μ is viscosity (with the subscript G, L and w representing vapor, liquid and water, respectively), h_{LG} is the latent heat of vaporization, g is gravitational acceleration, F is the particle shape factor (actual area of a particle/actual area of an equal-volume sphere) and ϵ is porosity. Equation [6] appears to satisfactorily represent the present data. On the other hand, [4], with $C = 1.075$, corresponding to the data of figure 9, grossly overpredicts the present dryout data. It is used, in the present derivation, nevertheless, because the result, [5], is independent of C, and under the assumption that factors affecting the absolute value of q_{cr} will be principally reflected in the intercept C rather than the slope of the flooding line.

4.2. The saturation profile

Before the prediction of the saturation profile, a model which can predict the incipient dryout data obtained in the present experiment must be developed. The reason is that saturation profiles will depend on the relative permeabilities in the bed, and the event of dryout inception can be used as a sensitive benchmark for them. The approach is along the lines suggested by Lipinski (1982). The model for counter-current flow is

$$-\frac{dP}{dz} = \rho_G g + \frac{\rho_G}{\eta\eta_G} J_G^2 + \frac{\mu_G}{\kappa\kappa_G} J_G \quad [7]$$

and

$$-\frac{dP}{dz} = \rho_L g - \frac{\rho_L}{\eta\eta_L} J_L^2 - \frac{\mu_L}{\kappa\kappa_L} J_L. \quad [8]$$

The pressure drop, the term on the l.h.s., is balanced by the gravitational force, the first term on the r.h.s., and the drag forces in these equations. The second term on the r.h.s. is the drag force for turbulent flow and the third term is that for laminar flow. The capillary pressure is neglected here. The interfacial drag between liquid and vapor reported by Ginsberg (Tutu *et al.* 1983) is introduced through the relative permeabilities: the permeability of laminar flow, κ, suggested by Blake & Kozeny (see Scheidegger 1960) and the permeability of turbulent flow, η, suggested by Burge & Plummer (see Scheidegger 1960) are chosen as

$$\eta = \frac{\epsilon^3 d}{1.75(1-\epsilon)} \quad [9]$$

and

$$\kappa = \frac{\epsilon^3 d^2}{150(1-\epsilon)^2}. \quad [10]$$

The general form of the relative permeabilities suggested by Hofmann & Schulenberg (1983) is selected, i.e.

$$\eta_G = (1-s)^n, \quad [11]$$

$$\eta_L = s^n, \quad [12]$$

$$\kappa_G = (1-s)^m \quad [13]$$

and

$$\kappa_L = s^m. \quad [14]$$

By eliminating the pressure drop term in [7] and [8] and introducing continuity and energy equations, [2] and [3] with $\Delta m' = 0$, we can derive the following algebraic equation:

$$\frac{q^2}{\eta h_{LG}^2}\left(\frac{1}{\rho_G \eta_G} + \frac{1}{\rho_L \eta_L}\right) + \frac{q}{\kappa h_{LG}}\left(\frac{\mu_G}{\rho_L \kappa_L} + \frac{\mu_G}{\rho_L \kappa_L}\right) + (\rho_G - \rho_L)g = 0. \quad [15]$$

Since heat losses have been neglected, there will be no heat which can be removed when only vapor or only liquid exist at the top layer ($s = 0$ or $s = 1$). A maximum value of q exists with respect to s and it should be q_{cr}. Therefore, q_{cr} was determined by maximizing q with respect to s at the top of the bed numerically. The predictions of q_{cr} are compared with the experimental data obtained in the present experiment in figure 11. Based on the data, m and n were chosen as 3 and 6, respectively. Also, a value of 4.5 mm as the characteristic size of particles was used in the calculation. This value was obtained from [9] with the permeability of turbulent flow measured in the present experiment. Note that this prediction did not make use of CHF correlation [6].

After the correct relative permeabilities were developed from the present data, the saturation profile could be predicted. The quasi-steady-state approach suggested by Hofmann & Schulenberg (1983) was employed here. The depletion rate can be seen as a fictitious vapor mass flux added from the bottom of an imaginary bed which has a height of $(H - z_{id})$, where z_{id} = dryout inception position. The depletion rate is constant over this height. The depletion rate, hence, can be predicted by [5]. The saturation profiles were obtained by carrying out the following steps: (a) the dp/dz term is eliminated between [7] and [8] to obtain a relationship between J_G and J_L; (b) J_L is eliminated from this result by using [2] and [5]; and (c) J_G is eliminated from this result by using [3]. Finally, the heat fluxes at any z are expressed in terms of the equivalent power densities, i.e.

$$q = zQ \quad [16]$$

to obtain a quadratic expression for z in terms of the local saturation s. The calculation is performed by a computer.

The saturation curves at different stages for a step increase in the heat flux q from 0.5 q_{cr} to 1.1 q_{cr} are shown in figure 12. The saturation curve shifts from I to II, when water is expelled from the bed due to the increase in the steam flow rate. Curve II is reached when the steam flow rate is fully established in the bed corresponding to 1.1 q_{cr}. This curve is unstable because of the imbalance of the incoming water flow rate and the outgoing steam flow rate. The saturation curve continuously

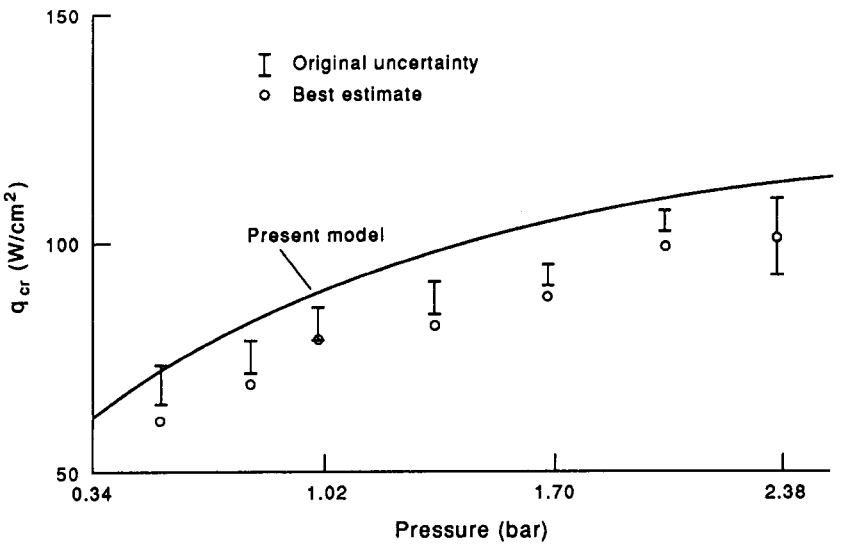

Figure 11. Comparison of the predictions of the present model and the incipient dryout data obtained in the present experiment.

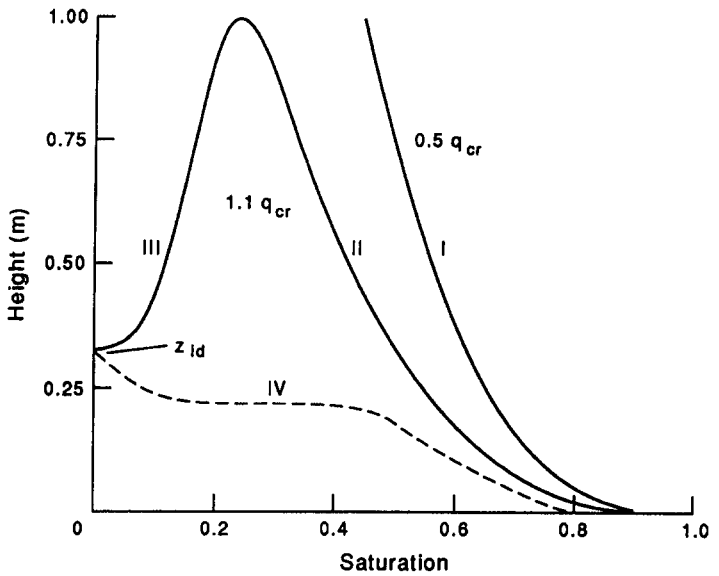

Figure 12. The saturation profiles and transitions for a heat flux increase from $0.5q_{cr}$ to $1.1q_{cr}$.

shifts to the left as the water inventory in the bed decreases until it eventually touches the zero saturation line, somewhere inside the bed, say at z_{id}, as shown in figure 12. At this time the saturation profile above z_{id} is shown as curve III, which is the other branch of curve II. Below z_{id}, the profile is shown schematically as curve IV, which cannot be computed without a fully transient analysis.

4.3. Estimation of DDT and CEL

DDT can be estimated by the time period in which the saturation curve shifts from II to III, since the process I–II will be completed in only a few seconds:

$$\text{DDT} = \frac{\rho_L V_{Ld}}{A\Delta m'}. \qquad [17]$$

The liquid volume being depleted in the bed before dryout, V_{Ld}, is derived from the area A_{Ld} between saturation curves II, III and IV as

$$V_{Ld} = A_{Ld}\epsilon A. \qquad [18]$$

Unfortunately, the saturation curve IV is missing and only a transient model can provide this information. Nevertheless, a crude estimation of DDT can be made by the assumption that

$$\frac{V_P}{V_{Ld}} = \frac{H - z_{id}}{H}, \qquad [19]$$

where V_P is the liquid volume being depleted within the portion of the bed above z_{id} before dryout. It can be derived from the area A_P between saturation curves II and III above z_{id} as

$$V_P = A_P\epsilon A. \qquad [20]$$

DDT becomes

$$\text{DDT} = \frac{\rho_L V_P H}{A\Delta m'(H - z_{id})}. \qquad [21]$$

Using this expression in [1] together with the expression for q_{cr}, from [6], and $\Delta m'$, from [5], a value of E can be computed for each value of q, i.e. for each experimental run. These computed values (line marked $s_{di} = 0.0$) are compared with the experimental ones in figure 13. Although the predicted value of E is not constant, the steep slope of the prediction curve reflects the behavior of the constant energy line.

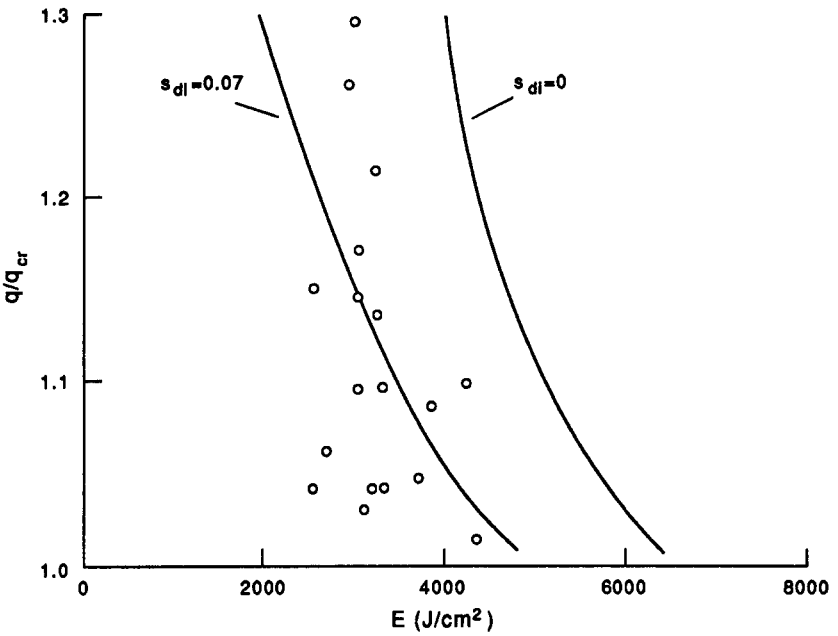

Figure 13. Theoretical prediction of the CEL behavior seen in the experiments; s_{di} is the saturation at dryout inception.

Figure 13 shows that the mean of the predicted E is different from that of the experimental data. The authors believe that the shift is due to the assumption of zero saturation corresponding to bed dryout. In reality, local dryout (liquid film breakup) is likely to occur before the saturation becomes exactly zero at z_{id} in the one-dimensional sense considered in the analysis. Therefore, the saturation s_{di} at dryout inception should not equal zero. By assuming that saturation curve III in figure 12 shifts to the right by 0.07, while maintaining its shape, the area A_P is reduced and the left curve in figure 13 is obtained, in better agreement with the data.

5. CONCLUSIONS

Experimental data, obtained at Purdue's Large Scale Corium Bed Simulation Facility, indicate that DDT is simply related to the applied power. The relationship, called the constant energy line (CEL), is useful to uniquely define the CHF, q_{cr}. It also provides a convenient and highly accurate means for the experimental measurement of q_{cr}. Based on these data the Theofanous–Saito (1981) correlation is recommended for the prediction of q_{cr} in deep beds of non-spherical coarsely-sized particulates. From simple mechanistic analysis it appears that the CEL behavior is related to coolant depletion phenomena because of flooding limitations during the pre-dryout transient. The final "steady state" (ignoring the eventual meltdown of the dryout portion) should consist of a top coolable zone with height $(H - z_{df})$ and a lower dry zone of height z_{df}. Considering the flooding limits this can simply be obtained from

$$\frac{z_{df}}{H} = 1 - \frac{q_{cr}}{q}.$$

Acknowledgements—The final support by the U.S. Nuclear Regulatory Commission under Contract No. NRC-03-83-093 is gratefully acknowledged. It is also our pleasure to thank Dr K. Iyer for many stimulating discussions leading to the final analytical interpretation of the CEL and Messrs J. Beecher and D. Reagan for helping with the experiment.

REFERENCES

BARLEON, L., THOMAUSKE, K. & WERLE, H. 1984 Cooling of debris beds. *Nucl. Technol.* **65**, 67–86.
BIRD, R. B., STEWART, W. E. & LIGHTFOOT, E. N. 1960 *Transport Phenomena*. Wiley, New York.

CATTON, I., DHIR, W. K. & SOMERTON, C. W. 1983 An experimental study of debris bed coolability under pool boiling conditions. EPRI Report No. NP-3094.

COMMONWEALTH EDISON COMPANY OF CHICAGO 1981 *Zion Probabilistic Safety Study.*

DHIR, V. K. & BARLEON, L. 1981 Dryout heat flux in a bottom heated porous layer. *Trans. Am. Nucl. Soc.* **38,** 385–386.

DHIR, V. K. & CATTON, I. 1977 Study of dryout heat fluxes in beds of inductively heated particles. U.S. Nuclear Regulatory Commission Report NUREG-0262.

GORHAM-BERGERON, E. 1983 Remaining uncertainties in predicting the coolability limits of a degraded reactor core. In *Proc. Int. Mtg on Light Water Reactor Severe Accident Evaluation*, Vol. 1, TS15.1. *Am. Nucl. Soc.*, Cambridge, Mass.

HOFMANN, G. 1982 On the location and mechanisms of dryout in top-fed and bottom-fed particulate beds. In *Proc. 5th Post Accident Heat Removal Information Exchange Meeting, Post Accident Debris Coolability* (Edited by MULLER, U. & GUNTHER, C.). Braun, Karlsruhe.

HOFMANN, G. & SCHULENBERG, T. 1983 A quasi-steady-state approximation to the transient dryout behavior in debris beds. Presented at the *July Mtg on LWR Severe Accident Evaluation*, Cambridge, Mass.

HU, K. 1985 Coolability on a coarse corium debris bed. Ph.D. Dissertation, Purdue Univ., W. Lafayette, Ind.

HU, K. & THEOFANOUS, T. G. 1986 Scale effects and structures of the dryout zone in debris bed coolability experiments. In *Proc. 6th Information Exchange Mtg on Debris Coolability*, Univ. of California, Los Angeles, p. 24–1.

HU, K., GHERSON, P. & THEOFANOUS, T. G. 1984 The large scale simulation of debris bed coolability. *AIChE Symp. Ser.* **80236,** 380–384.

JAKOBSSON, J. O., CATTON, I. & SQUARER, D. 1983 The pressure dependence on dryout heat flux. In *Proc. Int. Mtg on Light Water Reactor Severe Accident Evaluation*, p. 18.4–1. Am. Nucl. Soc., Cambridge, Mass.

LIPINSKI, R. J. 1982 A model for boiling and dryout in particle beds. Sandia National Labs Report NUREG/CR-2646.

LIPINSKI, R. J. 1983 A review of debris coolability models. In *Proc. Int. Mtg on Light Water Reactor Severe Accident Evaluation*, Am. Nucl. Soc., Cambridge, Mass.

MARSHALL, J. S. & DHIR, V. K. 1983 On the counter-current flow limitations in porous media. In *Proc. Int. Mtg on Light Water Reactor Severe Accident Evaluation*, Vol. 2, pp. 18.5-1–18.5-7. Am. Nucl. Soc., Cambridge, Mass.

OSTENSON, R. W. & LIPINSKI, R. J. 1981 A particle bed dryout model based on flooding. *Nucl. Sci. Engng* **79,** 110–112.

SCHEIDEGGER, A. E. 1960 *The Physics of Flow through Porous Media.* Univ. of Toronto Press, Toronto.

SCHROCK, V. E., WANG, C-H., REVANKAR, C., WEI, L-H., LEE, S. Y. & SQUARER, D. 1984 Flooding in particle beds and its role in dryout heat flux prediction. Presented at the *6th Exchange Mtg on Debris Coolability*, Univ. of California, Los Angeles.

SOMERTON, C., CATTON, I. & THOMPSON, L. 1981 An experimental investigation into dryout in deep debris beds. Report ASME 81-WA/HT-17.

SOWA, E., HESSON, J., GEBNER, R. & GOLDFUSS, G. 1971 Heat transfer experiments through beds of UO_2 in boiling sodium. *Trans. Am. Nucl. Soc.* **142,** 725.

SQUARER, D., PIECZYNSKI, A. T. & HOCHREITER, L. E. 1982 Effect of debris bed pressure, particle size and distribution on degraded nuclear reactor core coolability. *Nucl. Sci. Engng* **80,** 2–13.

STEVENS, G. F. & TRENBERTH, R. 1982 Experimental studies of boiling heat transfer and dryout in heat generating particulate beds in water at 1 bar. Presented at the *5th PAHR Information Exchange Mtg*, Karlsruhe, Germany.

THEOFANOUS, T. G., GHERSON, P., NOURBAKHSH, H. P., HU, K., IYER, K., VISKANTA, R. & LOMMERS, L. 1983 LWR and HTGR coolant dynamics: the containment of severe accidents. U.S. Nuclear Regulatory Commission Report NUREG/CR-3306.

THEOFANOUS, T. G. & SAITO, M. 1981 An assessment of class-9 (core-melt) accidents for PWR dry-containment systems. *Nucl. Engng Des.* **66,** 301–332.

TUTU, N. K., GINSBERG, T. & CHEN, J. C. 1983 Interfacial drag for two-phase flow through high permeability porous beds. Brookhaven National Labs Report BNL-NUREG-32950.